Spectrum of Engineering Sciences
ISSN (e) 3007-3138 (p) 3007-312X Volume 3, Issue 12, 2025

Performance Optimization of 132 KV Electrical Power Grid Station

M. A. Raza[*1], Muhammad Shahid[2], Darakhshan Ara[3], Fatima Tul Zuhra[4]

*[*1]Department of Electrical Engineering, Mehran University of Engineering and Technology, SZAB Campus Khairpur Mirs' Sindh Pakistan*
[2]Department of Data Science, Dawood University of Engineering and Technology, Karachi, Pakistan
[3]Department of Basic Sciences and Humanities, Dawood University of Engineering and Technology. Karachi, Pakistan
[4]Department of Information Technology, Shaheed Benazir Bhutto University Sanghar Campus

[*1]amirraza@muetkhp.edu.pk

DOI: https://doi.org/10.5281/zenodo.19592012

Keywords
Power system stability, grid station, load flow, short circuit, transient stability.

Article History
Received: 20 October 2025
Accepted: 30 November 2025
Published: 15 December 2025

Corresponding Author: *
M. A. Raza

Abstract
A case study of 132 KV grid station is under taken for improving the reliability, stability, and also for efficient operation of the power system. Electrical Transient Analyzer Program (ETAP) software is used to model the study which covers the three major aspects of power system such as Load Flow Analysis (LFA), Short Circuit Analysis (SCA), and Transient Stability Analysis (TSA). LFA identified under voltage and transformer overloading occurrences in the system. As a solution to these problems, a Static VAR Compensator (SVC) system was then incorporated in order to enhance voltage stability, decrease transformer loading and active and reactive power losses. SCA is used to assess the fault tolerance of the system by simulating different fault scenarios such as Line-to-Grounded (LG), Line-to-Line (LL), Double Line-to-Ground (LLG) and Three-phase (3Φ) faults. The results provided valuable information that enabled adequate understanding of fault currents and protective device coordination for safe and reliable system operation. The dynamic response of the system to disturbances, such as faults and recovery scenarios, will be assessed through TSA. The key parameters of the analysis were observed over a time interval of 60 seconds, which proved system stability under fault recovery, and provided important data for stability improvement in the future. This study not only overcame the current operational obstacles but also led to the optimization of the performance of substations.

I. INTRODUCTION

Nowadays, the modern societies' have growing energy demand and also require reliable and stable electric power that can be managed well [1]. As far as electricity distribution is concerned, substations play a key role, they are junctions where voltage levels can be adjusted, the power is monitored and controlled [2]. Good management of substations in turn maintains healthy power flows, keeps voltage stable, and lowers the risk of system breakdowns. It adds up to a more robust electricity grid [3]. The increasing complexity of power networks, combined with the promotion and integration of non-conventional power sources like wind and solar power have placed new demands on substations [4]. They are asked today to keep up performance standards in the face of load changes, to manage faults and other transient disturbances more effectively. This can be seen from their importance as network control points during grid outages [5].

Power flow study or load flow analysis is a calculation of steady-state operating conditions of a 132 kV grid station, such as determining the magnitude of voltages, phase angles, active and reactive power flows and losses across buses and lines. In a case of a 132 kV grid station which is a critical interconnection point of transmission lines and distribution networks, this analysis will provide balanced power distribution during both normal and contingency cases. Short circuit analysis measures fault currents (3 phase, single-line-to-ground, line-to-line) at a 132 kV grid station to determine the withstand of circuit breakers, transformers, busbars, and insulators. The transient stability of a 132 kV grid station after significant events such as three phase faults, line trips, or generator trips is considered in terms of rotor angle swings and power-angle curves during the initial 2-10 seconds.

A case study of 132 KV substation is under taken that represents an important infrastructure. This substation undergone a stringent testing process and a comprehensive receiving inspection, and it operates reliably at high voltages [6]. It supplies electricity over a wide area including industrial, commercial, and residential areas. The substation must therefore be operated effectively if it is to ensure that customers have a reliable electric power supply particularly in regions which have experienced rapid economic growth, for large increases in electricity demand [7]. However, the substation is confronted with several operational problems such as voltage instability, transformer overloading, losses throughout the power system and potential faults. These problems require careful analysis to discover their causes and suggestions for solving them in way that will raise substation operational efficiency [8].

To cope with the sub-station failure challenges, ETAP software has been introduced into this research. ETAP is an electrical network analysis and simulation program providing a full range of analysis functions, including LFA, SCA and TSA calculations. By modeling the 132 KV substation in ETAP, this paper is intended to analyze the various operational modes of the substation and propose methods to improve its performance and to identify the critical concerns and provide solutions to optimize the performance of the 132 KV substation. The specific goals are:

1. To simulate the power system substation of 132 KV using ETAP software and to perform the LFA, SCA and TSA.
2. To overcome the under-voltage problem, minimize the losses of power system and also to improve the power factor of the system.

II. Research Methodology

A 132 kV to 11 KV substation is an important substation of the electrical supply system which plays a great role in providing safe, reliable, and efficient supply of electricity from the electricity transmission network of high voltage to the electricity distribution network of medium voltage. Every element in the substation has its specific purpose as well as its contribution to efficiency and stability of the system. The research flow diagram of the proposed work is shown in Figure 1 and the single line diagram of 132 KV substation is presented in Figure 2.

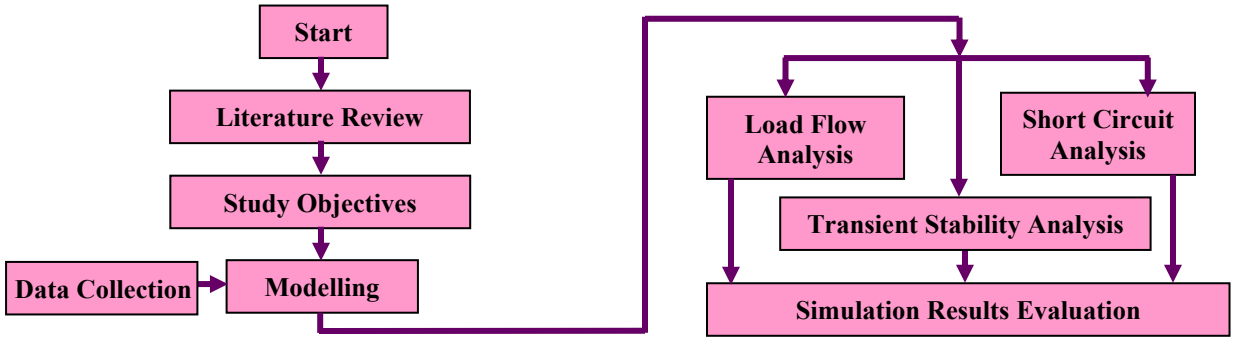

Figure 1: Flow chart of the proposed methodology

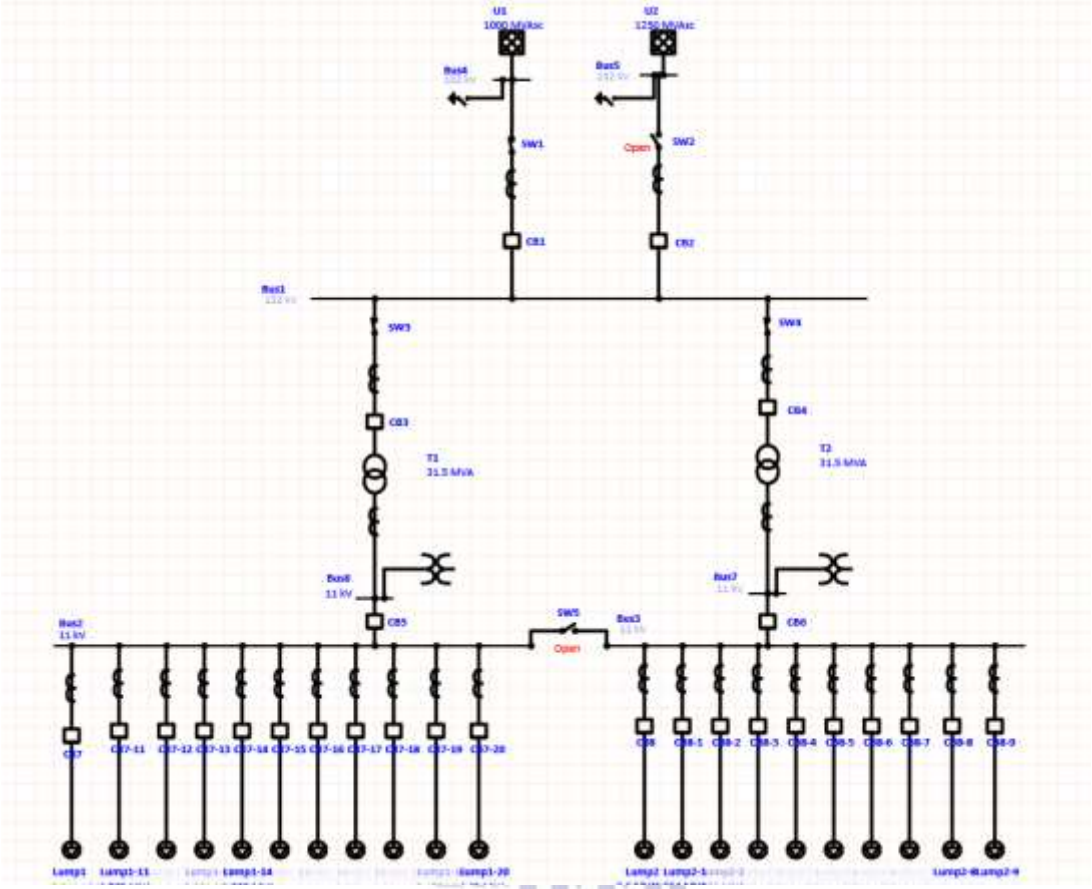

Figure 2: Single line diagram of substation modeled in ETAP

A. Load Flow Analysis (LFA)

The basic objective of the LFA is to determine the bus voltages, power flows, and checks systems limits and losses. Further, the elements of power systems for LFA like simple bus, slack or swing bus, voltage-controlled buss, real and reactive buss, transmission lines and generators. The power system is modeled through a set of standards, which captures the bilateral flow of power between nodes, or buses. These equations have been obtained from Kirchhoff laws of electrical circuit [9]. Power at any bus in the network is the total power that either enters or exits the bus in the network. The relationship between the power, voltage, and admittance matrix is expressed in Eqn. (1) [10]:

$$P_i = V_i \sum_{j=1}^{n} Vj \ \left(G_{ij}\, cos\theta_{ij} + B_{ij} sin\theta_{ij}\right) \quad Eqn.\,(1)$$

Where, P_i is the active power injected into bus i, V_i and V_j are the voltages at buses i and j, respectively. G_{ij} and B_{ij} are the real and imaginary parts of the bus admittance matrix (Y-bus matrix), which represent the system's conductance and susceptance between buses i and j. $\theta_{ij} = \theta_i - \theta_j$ is the phase angle difference between bus i and bus j. The Eqn. (2) shows the reactive power injection [11].

$$Q_i = V_i \sum_{j=1}^{n} Vj \ \left(G_{ij}\, sin\theta_{ij} - B_{ij}\, cos\theta_{ij}\right) \quad Eqn.\,(2)$$

Where, Q_i is the Reactive power injected into bus i. The above equations are applied for each bus hence giving a system of non-linear equations and are solved for voltage magnitudes Vi and angles θi at each bus.

The Y-bus or the admittance matrix is one of the most important matrices used in LFA calculations, it exhibits the admittances of the network between the buses. An N-bus system has an N x N Y-bus matrix of which each yij is the admittance between bus i and bus j and it is expressed in Eqn. (3) [12]:

$$Y_{ij} = G_{ij} + jB_{ij} \qquad Eqn.(3)$$

Where, G_{ij} is the conductance, and B_{ij} is the susceptance between bus *i* and bus *j*.

B. Short Circuit Analysis (SCA)

Electricity equipment's like generators, transformers, and transmission lines are rated to specific voltage and current values. The increase in the fault currents can exceed the ratings of equipment, which can damage the equipment. This process of estimating the potential fault currents is known as SCA and it serves to caution that protective devices (typically circuit breakers, relays, etc.) are sized and coordinated accordingly. There are different types of faults [13]:

1. Three Phase Fault: The worst fault type in terms of the magnitude of the current. It happens when the three phases are short-circuited, and it is usually the fault with the highest current in the system.
2. Line-to-Line Fault: When two phases are short-circuited together; bypassing the load and allowing direct current flow between two lines.
3. Line-to-Ground Fault: When a single phase touches the ground, meaning that current flows from the phase directly to ground.
4. Double Line-to-Ground Fault: When two phases are shorted at the same time to ground.

Out of these faults, the three-phase fault is symmetrical, but the rest are asymmetrical faults. Symmetrical faults include all three phases alike that means same current passing through all three phases while in asymmetric faults there is less current in one or two phases [14].

The thevenin equivalent circuit reduces the complex network to a voltage source and impedance (thevenin impedance) for short circuit analysis. This makes it easier to calculate the fault currents. The formula for calculating the fault current is shown in Eqn. (4) [15]:

$$I_f = \frac{V_{pre-fault}}{Z_{total}} \qquad Eqn.(4)$$

Where: I_f is the fault current, $V_{pre-fault}$ is the voltage at the fault location before the fault occurs (often the nominal system voltage). Z_{total} is the total impedance between the source and the fault location.

To understand the system's response to different types of faults, it's essential to compute the short circuit current using symmetrical components. Symmetrical components decompose unbalanced sets of phasors (in case of faults) into three balanced sets [16]:

1. Positive sequence components (I_1): Represent the normal operating conditions.
2. Negative sequence components (I_2): Represent the imbalance caused by faults.
3. Zero sequence components (I_0): Represent current flow through the neutral in case of grounding faults.

The total fault current is the sum of these components.

For a three-phase balanced fault, the system is analyzed using the positive sequence network only. The fault current is given in Eqn. (5) [17]:

$$I_f = \frac{V}{Z_1} \qquad Eqn.(5)$$

Where: V is the pre-fault line-to-neutral voltage at the fault point. Z_1 is the positive sequence impedance seen from the fault point.

For a line-to-line fault involving phases A and B, the current through the fault is given in Eqn. (6) [18]:

$$I_f = \frac{V}{Z_1 + Z_2} \qquad Eqn.(6)$$

Where: Z_1 is the positive sequence impedance. Z_2 is the negative sequence impedance.

For a single line-to-ground fault, the fault current is determined using all three sequence networks (positive, negative, and zero) as shown in Eqn. (7) [19]:

$$I_f = \frac{V}{Z_1 + Z_2 + Z_0} \qquad Eqn.(7)$$

Where: Z_1, Z_2, and Z_0 are the positive, negative, and zero sequence impedances, respectively.

For a double line-to-ground fault (involving two phases and ground), the fault current is shown in Eqn. (8) [20]:

$$I_f = \frac{V}{Z_1 + Z_2 + \frac{Z_0}{2}} \qquad Eqn.(8)$$

Where: Z_1, Z_2, and Z_0 are the positive, negative, and zero sequence impedances, respectively.

The use of symmetrical components is key to analyzing unbalanced faults in power systems. The idea is to decompose the unbalanced system into balanced sets that can be solved using simpler

techniques. Symmetrical components allow for the decoupling of the power system equations into three independent systems: the positive, negative, and zero sequence networks [21]:

C. *Transient Stability Analysis (TSA)*

When a large disturbance occurs in the system, such as a fault, the generators in the system may lose synchronism, leading to system instability. The analysis aims to determine whether the generators can remain synchronized with each other after the fault is cleared and if the system can settle into a new stable operating condition [22]. Transient stability is determined by analyzing the system's behavior over a short period (seconds to a few minutes) after the disturbance occurs. During this period, the system undergoes rapid changes in generator rotor angles and power flows [23].

The primary focus of transient stability analysis is rotor angle stability, which concerns the relative motion of interconnected generators in the power system. If the rotor angles between generators increase beyond a certain threshold, the system may lose synchronism, leading to instability [24].

The transient stability of synchronous generators is governed by the swing equation, which describes the rotor's angular motion during and after a disturbance. The equation is derived from Newton's second law of motion, where the unbalanced torque acting on a generator's rotor is responsible for changes in its angular velocity. The swing equation for a single synchronous generator is given in Eqn. (9) [25]:

$$M \frac{d\delta^2}{dt^2} = P_m - P_e \quad Eqn.(9)$$

Where: M is the generator's inertia constant (in MWs), representing the kinetic energy stored in the rotating mass. δ is the rotor angle of the generator, representing the angular displacement with respect to a reference. $\frac{d\delta^2}{dt^2}$ is the angular acceleration. P_m is the mechanical power input to the generator (from the prime mover, such as a turbine). P_e is the electrical power output of the generator (supplied to the grid).

The difference between the mechanical input power (P_m) and the electrical output power (P_e) results in an accelerating or decelerating torque that causes changes in the rotor angle δ. If the system remains stable, the rotor angle will settle into a new equilibrium point after the disturbance.

For a multi-machine system, transient stability is more complex, as multiple generators interact dynamically. The swing equation for each generator is coupled with others through the power system network. The stability of the entire system is dependent on the relative motion of all generators in the system. The swing equation for each generator i in a multi-machine system is given in Eqn. (10) [26]:

$$M_i \frac{d\delta_i^2}{dt^2} = P_{m,i} - P_{e,i} \quad Eqn.(10)$$

Where: M_i is the inertia constant of generator i. δi is the rotor angle of generator iii relative to a reference. $P_{m,i}$ and $P_{e,i}$ are the mechanical input and electrical output powers for generator i, respectively. The electrical power $P_{e,i}$ depends on the power flows through the network, which are determined by the voltages, impedances, and rotor angles of all other generators.

III. Results and Discussion

The simulation results of 132 KV electrical power grid station based on the load flow, short circuit and transient stability analysis is discussed in this section.

A. *Simulation Results of Load Flow Analysis*

Simulated model of the substation using ETAP software is given in Figure 2. After that LFA was performed without SVC to analyze the voltage conditions at the different buses and equipment present in the system as shown in Figure 3. This provided the insight of the system, where it gave us the ability to develop a list of the potential cases of under voltage and the manner in which different components of our system would behave as load conditions were changed. The analysis of these results would enable us to identify those parts of the substation that need boards/voltage strengthening in order to increase stability and reliability in the system. Furthermore, the LFA with SVC connected is shown in Figure 4. The detailed results of load flow analysis of the transformer and bus bars with and without SVC compensation is discussed in Table 1 and Table 2.

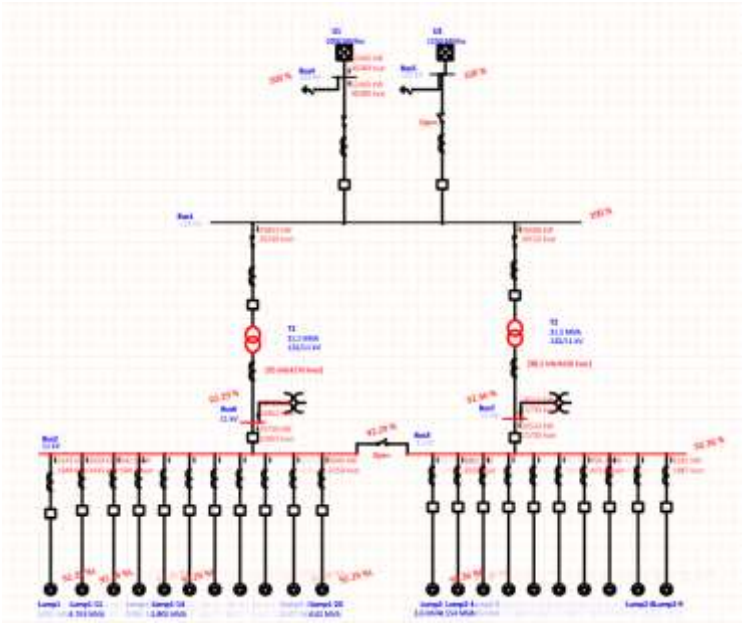

Figure 3: Shows the LFA results without SVC connected.

From the results, it is expected that the voltage profiles at buses 2, 3, 6 and 7 will improve significantly as a result of the connection of the SVC in parallel with buses. Moreover, it implies a better power factor for both transformers which reduces the total losses of the system thus makes it more efficient. Real-time dynamic reactive power adjustment plays a key role in stabilizing the system, making it possible for the system to maintain voltage levels up to the optimal operating levels in different loading conditions. Once implemented, a new load flow will be performed to analyze these improvements and to evaluate the performance of the system.

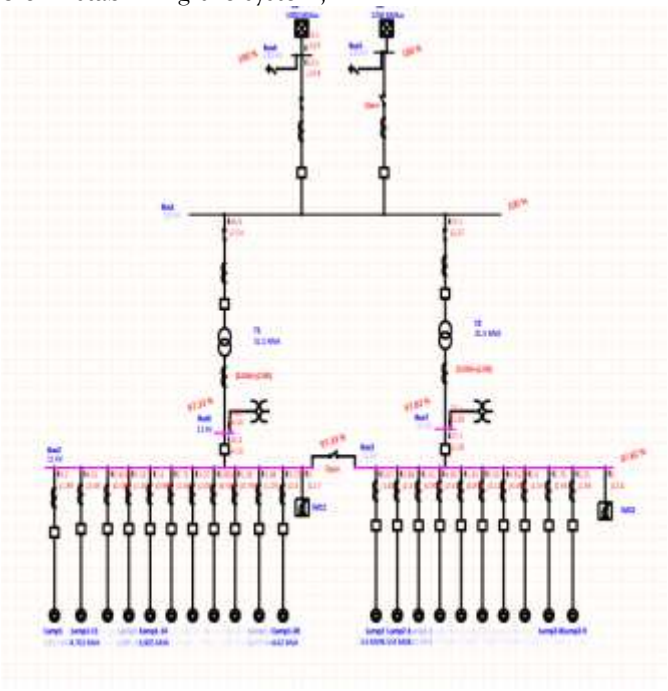

Figure 4: Shows the LFA results with SVC connected.

Table 1: Shows the LFA results of the transformers and bus bars, with and without SVC compensation

Equipment	Without SVC		With SVC	
	Ratings	% Loadings	Ratings	% Loadings
Transformer 1	31.5 MVA (132/33) kV	96.37	31.5 MVA (132/33) kV	84.7
Transformer 2	31.5 MVA (132/33) kV	97.78	31.5 MVA (132/33) kV	86.6
Equipment	Rated Value (kV)	Recorded Voltage (%)	Rated Value (kV)	Recorded Voltage (%)
Bus1	132	100	132	100
Bus2	11	92.29	11	97.33
Bus3	11	92.37	11	97.82
Bus4	132	100	132	100
Bus5	132	100	132	100
Bus6	11	92.29	11	97.33
Bus7	11	92.36	11	97.82

Table 2: Shows the results of load flow and losses with and without SVC

	LFA without SVC		LFA with SVC	
ID	T/F 1	T/F 2	T/F 1	T/F 2
KW flow	25756	26510	26264	27078
KVAr	15962	15730	4500	3280
Amp	1723	1752	1437	1463
% PF	85	86	98.5	99.2
% Loading	96.37	97.78	84.7	86.6
KW losses	0.193	0.193	0.135	0.135
KVAr losses	8.7	8.7	6.06	6.06

B. Simulation Results of Short Circuit Analysis

The results of an extensive short circuit analysis (SCA) of the 132kV substation modeled in ETAP, conducted to test the robustness of the system against faults and the effectiveness of the protection measures built into the system to isolate them. The four different types of fault conditions simulated, in the analysis, included Line-to-Ground (LG), Line-to-Line (LL), Line-to-Line-to-Ground (LL-G) and Three-Phase (3Φ) faults. The results of 3-Φ fault, LG fault, LL fault and LL-G fault in Figure 5, Figure 6, Figure 7 and Figure 8. Every class of fault involves a different operational issue which affects the stability of the system and the equipment differently as well. As expected, 3-Φ faults, the most severe, had the highest fault currents which posed serious threats to important components like transformers and breakers. On the other hand, LG faults, although not as catastrophic, pinpointed localized vulnerabilities and called for close monitoring and mitigation. The results showed that for LL and LL-G faults, intermediate fault current levels, confirm the asymmetry of the impact caused by unbalanced fault scenarios on the system. The comparative analysis of SCA in all faults is shown in Table 3.

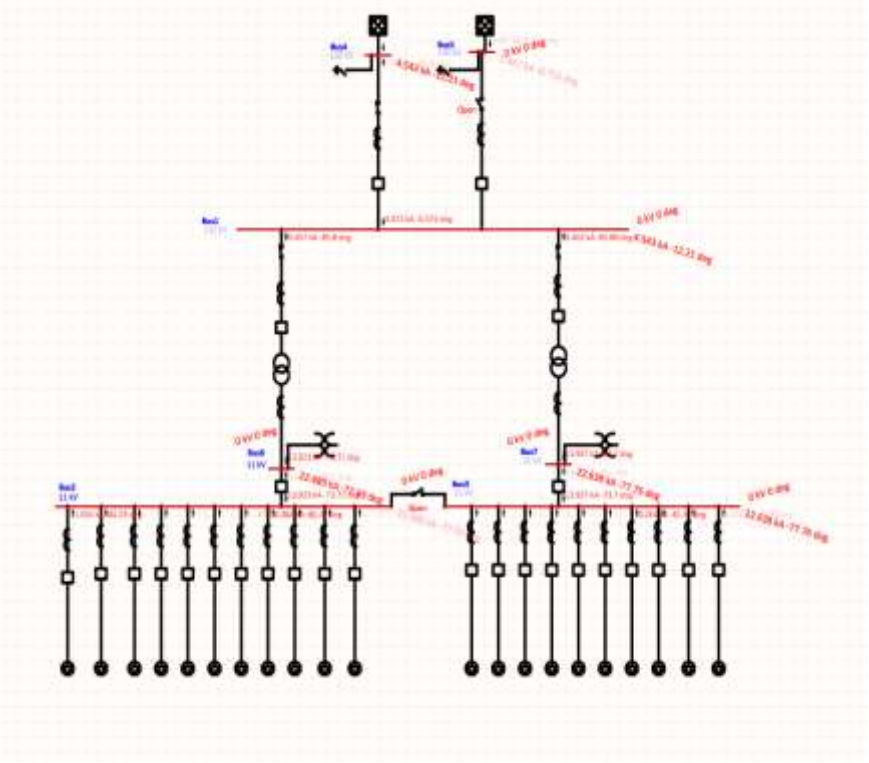

Figure 5: Shows the Three-Phase (3Φ) faults in Substation

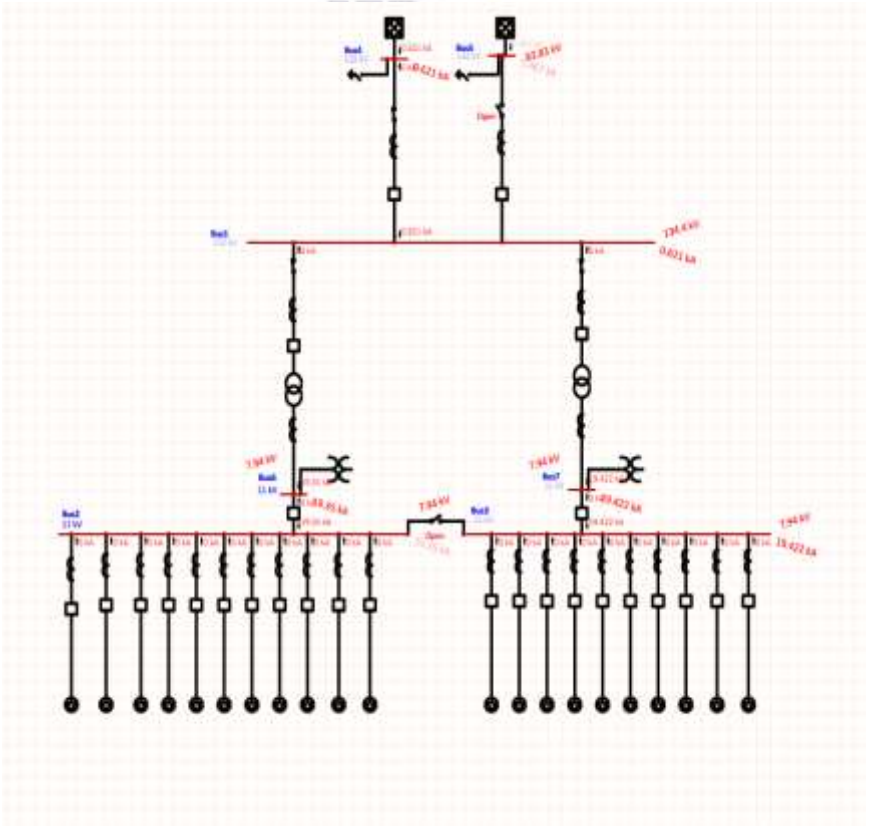

Figure 6: Shows the Line-to-Ground (LG) fault in Substation

Table 3: SCA results for all fault types

Bus		Fault Types			
Bus ID	KV	3-Φ	L-G	L-L	L-L-G
Bus 1	132	4.543	0.621	3.97	0.333
Bus 2	11	22.489	19.35	19.476	16.903
Bus 3	11	22.638	19.422	19.605	16.93
Bus 4	132	4.545	0.621	3.93	0.333
Bus 5	132	4.466	5.467	4.73	5.467
Bus 6	11	13.923	19.35	19.476	16.903
Bus 7	11	13.927	19.422	19.605	16.93

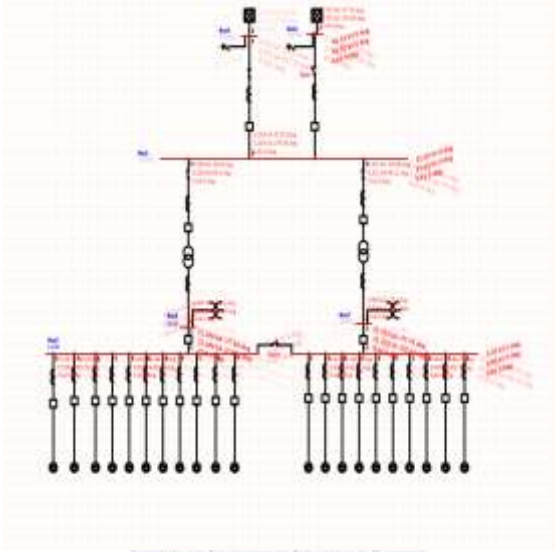

Figure 7: Shows the Line-to-Line (LL) fault in Substation

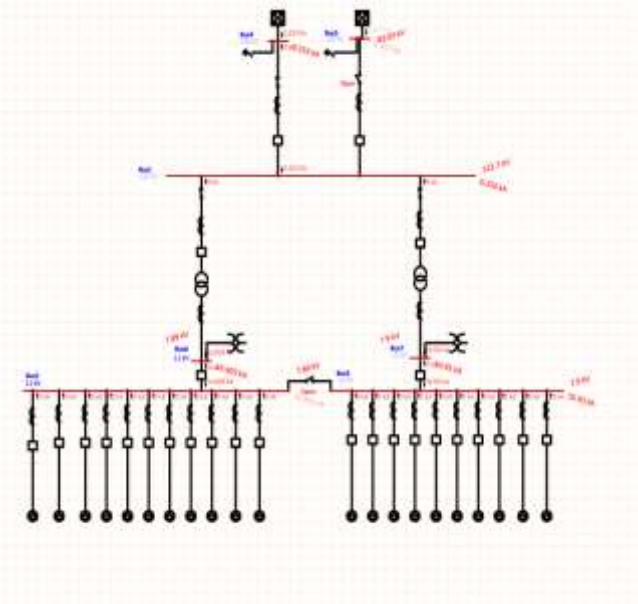

Figure 8: Shows the Line-to-Line-to-Ground (LL-G) fault in Substation

C. Simulation Results of Transient Stability Analysis

This transient stability analysis of 132kV substation system using ETAP was performed and analysis was made about whether the system remains synchronized or not under dynamic conditions (disturbances). The behavior of substation before the fault occurs is shown in Figure 9. Then study simulated faults at certain buses and created a fault event in 3.9 seconds of system execution. The fault continued to exist for a specific time, followed by this, fault clearance was simulated at 4.6 seconds, as done by different protective devices. The system response was evaluated over 15 seconds of total simulation time, enabling a detailed evaluation of the dynamics of recovery after the fault. The behavior of substation during the fault and after the fault is shown in Figure 10 and Figure 11.

Furthermore, transient stability analysis is one of the important studies since it gives explanations about how a power system reacts due to sudden disturbances (e.g. short circuits, loss of generation, rapid load change, etc.) in the power system. The metrics including rotor angle difference, frequency in the system, and bus voltage results over the network from the fault duration and recovery phase were extracted in this simulation. A large disturbance was created due to this fault which can be easily seen in rotor angles and voltage levels. However, the system started its recovery procedure when the fault was cleared at 4.6 seconds. The results showed how different system components and time components restore system balance, such as generators, loads, and transmission lines.

Over the 15 seconds, transient oscillations could be identified, and it could be seen whether the oscillations were being damped out. Rotor angle of generators be synchronized in stable scenarios, showing that system would not be vulnerable of falling into cascade failure due to the disturbance. In cases of transient instability, the results of this study delineated demands for changes in the system, for example, improving fault-clearing mechanisms, upgrading protective devices, or adding items for stabilization, for instance, power system stabilizers (PSS). The results for transient stability analysis are shown in Figure 12, Figure 13 and Figure 14.

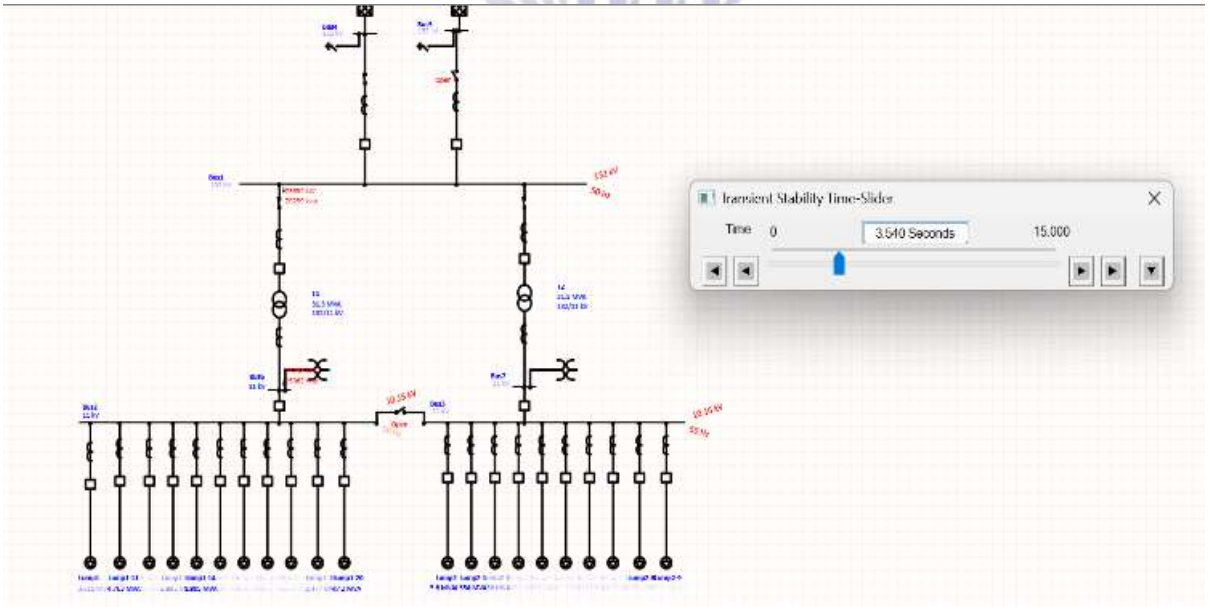

Figure 9: Shows the behavior of substation before fault occur

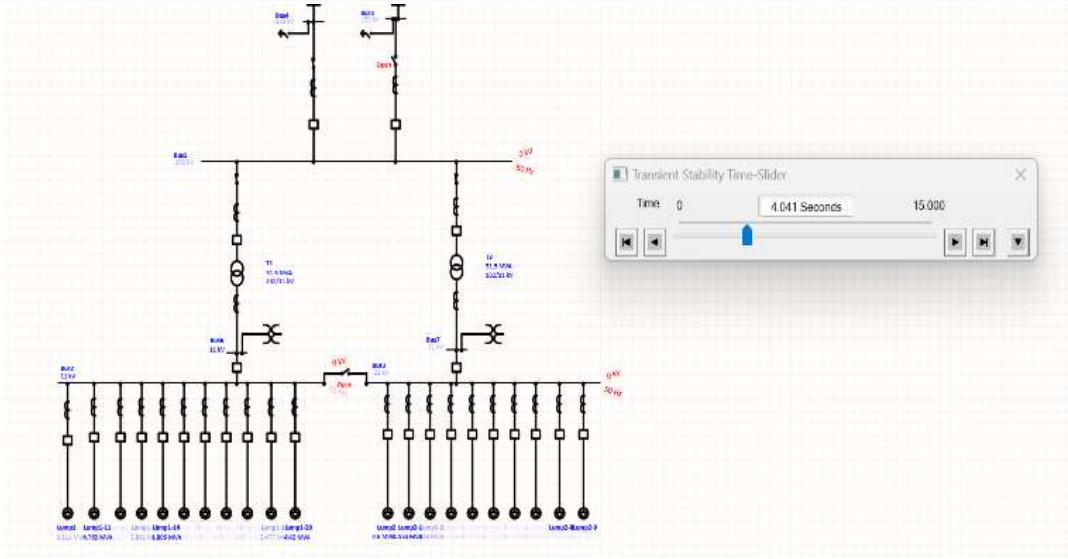

Figure 10: Shows the behavior of substation during fault occur

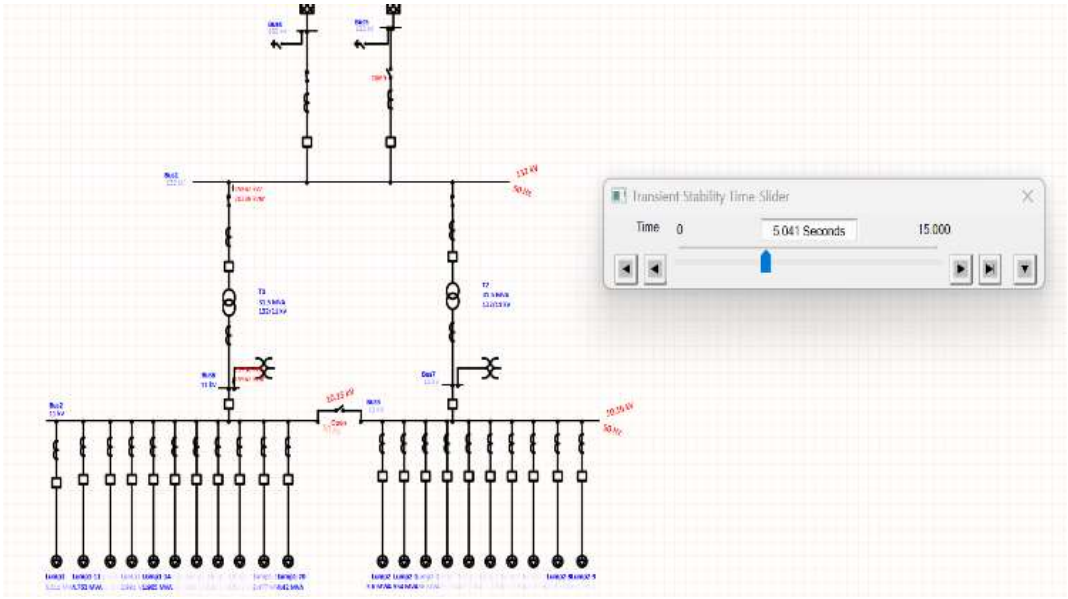

Figure 11: Shows the behavior of substation after fault occur

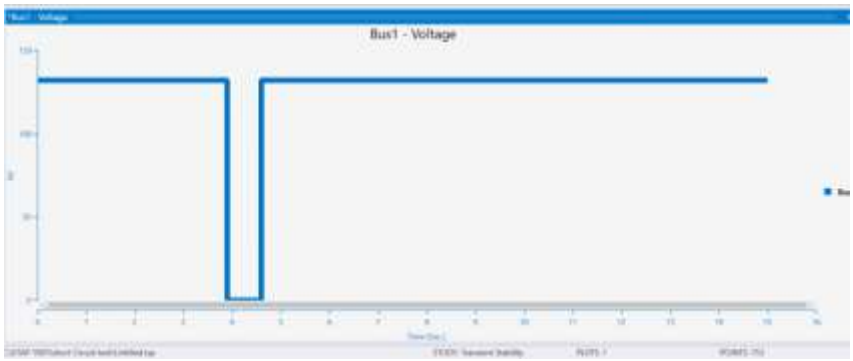

Figure 12: Shows the behavior of bus voltage before, during and, after fault occurrence

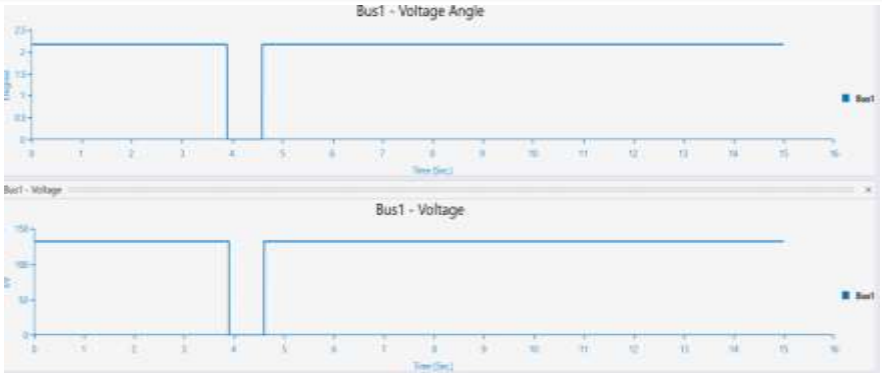

Figure 13: Shows the behavior of bus voltage and voltage angle before, during and, after fault occurrence

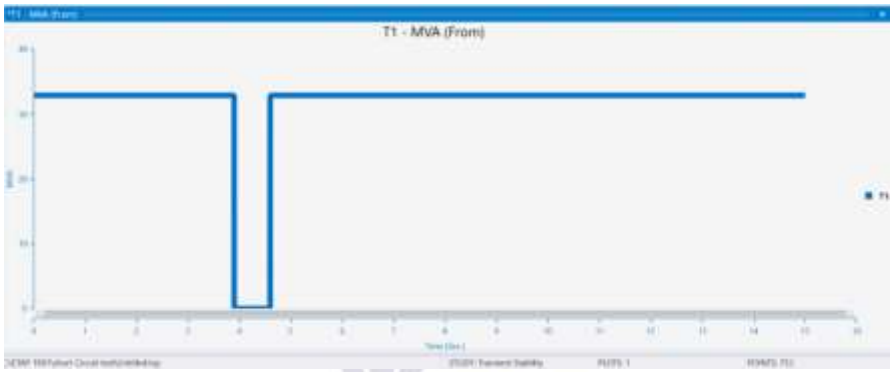

Figure 14: Shows the behavior of transformer 1 MVA before, during and, after fault occurrence

IV. CONCLUSION

This study is conducted on the 132 KV substation for the performance optimization. ETAP software is used to perform the LFA, SCA, and TSA and rectified key operational hurdles. The study shows how analyses of the power system can lead to improvements in voltage stability, transformer loading, power factor, fault tolerance and transient stability. The LFA was used to study voltage profile per bus, overloaded transformer, power factor, and total losses in steady state. SCA was performed to evaluate the fault tolerance of the system simulating different fault scenarios to evaluate the performance of the existing protective relays and the circuit breakers. TSA evaluated the system's response to large disturbances, particularly in terms of its capacity to remain in synchrony and reestablish stable voltage conditions.

Acknowledgement: Data will be made available upon the request

Conflict of Interest: The authors declare no conflict of interest.

V. REFERENCES

[1] P. Ray, P. K. Ray, and S. K. Dash, "Power quality enhancement and power flow analysis of a PV integrated UPQC system in a distribution network," *IEEE Transactions on Industry Applications*, vol. 58, pp. 201-211, 2021.

[2] B. Huang and J. Wang, "Applications of physics-informed neural networks in power systems-a review," *IEEE Transactions on Power Systems*, vol. 38, pp. 572-588, 2022.

[3] H. Bagheri Tolabi, A. Lashkar Ara, and R. Hosseini, "An enhanced particle swarm optimization algorithm to solve probabilistic load flow problem in a micro-grid," *Applied Intelligence*, vol. 51, pp. 1645-1668, 2021.

[4] S. Li, C. Gu, P. Zhao, and S. Cheng, "Adaptive energy management for hybrid power system considering fuel economy

and battery longevity," *Energy Conversion and Management*, vol. 235, p. 114004, 2021.

[5] S. Jamal, N. M. Tan, and J. Pasupuleti, "A review of energy management and power management systems for microgrid and nanogrid applications," *Sustainability*, vol. 13, p. 10331, 2021.

[6] B. Yang and S. Chang, "On-line monitoring and control of auxiliary facilities in substation," in *2021 3rd International Academic Exchange Conference on Science and Technology Innovation (IAECST)*, 2021, pp. 1931-1934.

[7] Y. Sun, X. Xie, C. Wu, W. Liu, and Q. Fan, "Research on operation and maintenance mode of digital substation based on fuzzy analytic hierarchy process," in *2023 7th International Conference on Green Energy and Applications (ICGEA)*, 2023, pp. 115-119.

[8] N. A. Azhar, N. A. M. Radzi, I. S. Mustafa, K. H. M. Azmi, F. S. Samidi, I. T. Zulkifli, *et al.*, "Selecting communication technologies for an electrical substation based on the AHP," *IEEE Access*, vol. 11, pp. 110724-110735, 2023.

[9] X. Lu, W. Ouyang, Z. Wang, and J. Zhou, "Optimal planning of HV/MV substation locations and sizes considering battery energy storage systems for peak shaving," *Electrical Engineering*, vol. 106, pp. 7633-7641, 2024.

[10] S. Poudel, G. D. Black, E. G. Stephan, and A. P. Reiman, "Admittance matrix validation for power distribution system models using a networked equipment model framework," *IEEE Access*, vol. 10, pp. 9108-9123, 2022.

[11] J. Zhang, P. Wang, and N. Zhang, "Distribution network admittance matrix estimation with linear regression," *IEEE Transactions on Power Systems*, vol. 36, pp. 4896-4899, 2021.

[12] M. Rayati, M. Bozorg, and O. Alizadeh-Mousavi, "Admittance matrix estimation of radial distribution grids using power and voltage magnitude measurements," *Electric Power Systems Research*, vol. 234, p. 110619, 2024.

[13] D. Jana, J. Patil, S. Herkal, S. Nagarajaiah, and L. Duenas-Osorio, "CNN and Convolutional Autoencoder (CAE) based real-time sensor fault detection, localization, and correction," *Mechanical Systems and Signal Processing*, vol. 169, p. 108723, 2022.

[14] B. Xiang, Z. Tang, Q. Zhang, J. Zhang, X. Jiang, W. Huang, *et al.*, "Current-limiting and recovery characteristics of resistive-type superconducting fault current limiters during quench-recovery-requench process," *IEEE Transactions on Applied Superconductivity*, vol. 33, pp. 1-11, 2023.

[15] Q. Pang, L. Ye, H. Gao, X. Li, Y. Wang, and T. Cao, "Multi-timescale-based fault section location in distribution networks," *IEEE Access*, vol. 9, pp. 148698-148709, 2021.

[16] M. Halihal and T. Routtenberg, "Estimation of the admittance matrix in power systems under Laplacian and physical constraints," in *ICASSP 2022-2022 IEEE International Conference on Acoustics, Speech and Signal Processing (ICASSP)*, 2022, pp. 5972-5976.

[17] R. Aazami, S. Esmaeilbeigi, M. Valizadeh, and M. S. Javadi, "Novel intelligent multi-agents system for hybrid adaptive protection of micro-grid," *Sustainable Energy, Grids and Networks*, vol. 30, p. 100682, 2022.

[18] J. Ding, Y. Wang, Y. Qin, and B. Tang, "Adaptive global noise suppression deep deconvolution for weak fault signature mining of aero-engine accessory casing," *IEEE Transactions on Instrumentation and Measurement*, vol. 73, pp. 1-13, 2024.

[19] M. Ma, X. Li, W. Gao, J. Sun, Q. Wang, and C. Mi, "Multi-fault diagnosis for series-connected lithium-ion battery pack with reconstruction-based contribution based on parallel PCA-KPCA," *Applied Energy*, vol. 324, p. 119678, 2022.

[20] T. Yang, G. Li, S. Yuan, Y. Qi, X. Yu, and Q. Han, "The LST-SATM-net: A new deep feature learning framework for aero-engine hydraulic pipeline systems intelligent faults diagnosis," *Applied Acoustics*, vol. 210, p. 109436, 2023.

[21] J. Andruszkiewicz, J. Lorenc, B. Staszak, A. Weychan, and B. Zięba, "Overcurrent protection against multi-phase faults in MV networks based on negative and zero sequence criteria," *International Journal of Electrical Power & Energy Systems*, vol. 134, p. 107449, 2022.

[22] Y. Huang, J. Zhang, G. Wang, and Z. Xu, "Transient stability analysis and improvement of isolated renewable energy bases with VSC-DC transmission," *CSEE Journal of Power and Energy Systems*, 2025.

[23] P. Ge, C. Tu, F. Xiao, Q. Guo, and J. Gao, "Design-oriented analysis and transient stability enhancement control for a virtual synchronous generator," *IEEE Transactions on Industrial Electronics*, vol. 70, pp. 2675-2684, 2022.

[24] A. Bahmanyar, D. Ernst, Y. Vanaubel, Q. Gemine, C. Pache, and P. Panciatici, "Extended equal area criterion revisited: A direct method for fast transient stability analysis," *Energies*, vol. 14, p. 7259, 2021.

[25] C. Luo, S. Liao, Y. Chen, and M. Huang, "Quantitative Transient stability analysis for parallel grid-tied grid-forming inverters considering reactive power control," *IEEE Transactions on Power Electronics*, 2025.

[26] P. Sarajcev, A. Kunac, G. Petrovic, and M. Despalatovic, "Artificial intelligence techniques for power system transient stability assessment," *Energies*, vol. 15, p. 507, 2022.